Using vertical areas in finite set model predictive control of a three-level inverter aimed at computation reduction

Alireza JA'AFARI[1,*]📷, **S. Alireza DAVARI**[2]📷, **Cristian GARCIA**[3]📷, **Jose RODRIGUEZ**[4]📷
[1]Department of Electrical Engineering, Shahid Rajaee Teacher Training University, Tehran, Iran,
[2]Department of Electrical Engineering, Shahid Rajaee Teacher Training University, Tehran, Iran,
[3]Department of Electrical Engineering, Universidad de Talca, Curico, Chile,
[4]Department of Engineering, Universidad Andres Bello, Santiago, Chile,

Abstract: In power electronics applications, finite set model predictive control (FS-MPC) has proven to be a viable strategy. However, due to the high processing power required, using this technology in multilevel converters is difficult. This strategy, which is based on predicting the behavior of the system for all conceivable states, has an issue with a numerous of possible switching states. A recent and useful strategy for dealing with the problem is the limiting of calculations based on triangle regions. Despite its success, this method has several limitations, including the computation required to locate the right triangle and the boundary modes. In this research, the vertical areas are used for the limiting of calculations. Not only determining the right zone is an easy task with this strategy, but the number of possible candidates is also reduced to two. Furthermore, the boundary mode will not occur.

In the proposed method, two key advantages can be seen in the discussion of reduction of calculations: (1) new zoning, which eliminates the calculations related to the slope of the lines. (2) The number of options placed in the cost function has been reduced to 2 candidates. Simulations are used to validate the approach, which is applied to a three-level neutral point clamped (NPC) inverter.

Key words: Multilevel inverters, finite set model predictive control, computation reduction

1. Introduction

Multilevel inverters are one of the most efficient topologies among different converters for medium voltage [1] and high voltage [2] applications. Various switching techniques, such as pulse width modulation (PWM) [3, 4] and model predictive control (MPC) [5, 6], have been used for multilevel inverters in recent decades.

The PWM method is commonly used in linear control approaches. There has been a lot of research into the differences between linear controls and predictive-based techniques. In general, the predictive method, particularly the finite set model predictive (FS-MPC) method, has yielded positive results in power electronics applications. Fast dynamics and the ability to consider the converter's nonlinear effects are two examples of the benefits that this method can provide. In this technique, a cost function is predicted for all of the inverter's possible voltage vectors, and the best solution is chosen based on the lowest calculation of the predicted cost function [7].

Despite the benefits indicated above, using FS-MPC to multilevel inverters increases the required pro-

---

*Correspondence: Correspondence: a.jaafari1994@gmail.com

cessing power because the number of potential solutions in these topologies grows, for example, a three-level inverter has 19 voltage vectors and 27 switching states [8]. As a result, decreasing the calculation of FS-MPC's time for multilevel applications has been a study topic in recent years.

There are 18 active vectors and a zero vector in a three-level inverter. A three-level inverter has 27 switching states as each of these vectors represents one or more switching states [8]. The computational time and computational burden for the processor rise when each of these vectors is incorporated into the cost function. For this reason, several methods have been proposed to reduce computational burden and computational time. The number of vectors in the cost function has been reduced in all of those techniques.

The described approaches can be classified into three groups in a broad sense:

1) Area-based methods,

2) Sequential cost function methods,

3) Lookup table-based methods.

Considering the vectors in the sector where the reference voltage is placed is the most basic way among the area-based strategies. As a result, the number of vectors that the cost function must investigate is reduced by one-sixth with this strategy [9]. However, in some cases, the reduction achieved by this way is insufficient. In [10], the method is modified by taking into account two zones and four-vectors in each sector. After identifying four-vectors, the reference vector's vertical and horizontal components are rounded up and down, and one of the four vectors is deleted. Finally, the cost function examines these three vectors. Though the number of feasible solutions are reduced to four, extra equations are required to find the useless solutions. The distances from the three end lines, sectors three, four, and five, are used in [11] to obtain even further vector reduction. Each triangle region is defined by a three-digit number in this method. A three-digit number depending on the distance from sector lines three, four, and five determines the location of the reference vector in this method. This value is calculated by comparing the numbers to the locations of the reference vector. Though the number of the vectors is reduced by this technique, the computation process is lengthy due to the computation of the three distances, determination of the three-digit numbers, and the comparison of them with each region number.

The cascading cost functions method fall into the second group. A cost function is used to eliminate several vectors in this technique. The final solution is then chosen or the modulation times are calculated using the second cost function. In [12], the torque cost function is used to select three preliminary candidates and the flux cost function is used to find the final solution among these three candidates. This method reduces the number of cost function predictions, but the number of torque and flux predictions remains the same as in the standard method. In order to save computation time, the sequential technique is utilized in [13] for a three-level flying capacitor inverter. The first cost function distinguishes between voltage vectors that can control the capacitor voltage. Finally, the current based cost function examines these vectors. The first cost function examines all of vectors in [14], and the three vectors that minimize the cost function are determined. To give the required modulation timing, each of these three vectors is allocated to a distinct cost function. For time optimization, the second cost function requires a lot of processing power.

A specified table is utilized to pick the possible candidates in the last category. The table is created using the control algorithm's parameters. In order to determine the final solution, the cost function will predict and test the results of the selected candidates. In [15], this technique is applied to the matrix converter. Based on the sectors of the input and output vectors, three vectors are chosen. For these three vectors, the cost

function is investigated. In [16], for the drive applications, a table is created depending on the torque and flux circumstances. Because of the effect of each voltage vector on the torque and flux, the table is generated. The table based method is more simplified by forming the table for the first sector and generalizing the outcomes for the other sector in [17, 18]. With less processing power, three possible solutions for the cost function will be determined. This method has two notable accomplishments:

1) Because there are three possible candidates, the cost function should only be predicted three times.

2) The process of finding these three candidates needs less processing power compared to the other methods because it is based on the lookup table and the table is only formed for the first sector.

Indeed, this method is a hybrid of area-based and lookup table-based approaches, with the area-based methods providing good dynamics and the lookup table-based technique providing ease of use.

Despite the benefits of the strategy presented in [17], there are two issues to be addressed:

1) When the voltage reference is at the boundary area between two sectors, the three selected candidates may change slightly.

2) In order to determine the associated triangle area, the slope of the dividing lines must be calculated.

In this study, a solution to the aforementioned issues is given. In truth, the utilization of triangular regions is at the basis of both issues. Instead of a triangular area, the vertical area is offered in this study. Candidates will not marginally alternate during the transition between two sectors if this strategy is used. Furthermore, the criteria for determining the relevant zone do not necessitate any additional slope calculations, resulting in a significant reduction in computation time. Finally, the number of possible candidates will be two instead of three, which will more reduce the computation time.

Reducing computing is a key point emphasized in this article. To achieve this, a solution with different zoning has been used. The use of this zoning causes two types of computational reductions. In the first case, there is no need to calculate the slope of the lines, and, in the second case, the number of candidates in the cost function is reduced to 2 candidates.

2. Basics of FS-MPC in three-level NPC inverter

The structure of a three-level NPC inverter is shown in Figure. 1. The load model is the basis of the FS-MPC. The relationship between the voltage and the current of a resistive-inductive load is the following equation (1) in the stationary frame. It's important to note that the voltage and current relationships in the three-phase system (abc) are carried over to the orthogonal system ($\alpha\beta$).

$$\vec{v} = R_L\vec{i} + L_L\frac{d\vec{i}}{dt} \tag{1}$$

where $\vec{v} = v_\alpha + jv_\beta$ and $\vec{i} = i_\alpha + ji_\beta$ represent the voltage and current of the load, respectively.

The next step current can be predicted using the discrete form of the model as follows:

$$\vec{i}_{k+1} = \vec{i}_k + \frac{t_s}{L_L}\left(\vec{v}_k - R_L\vec{i}_k\right) \tag{2}$$

where t_s is the sampling interval, and subscripts k and $k+1$ show the measured value and the predicted value, respectively.
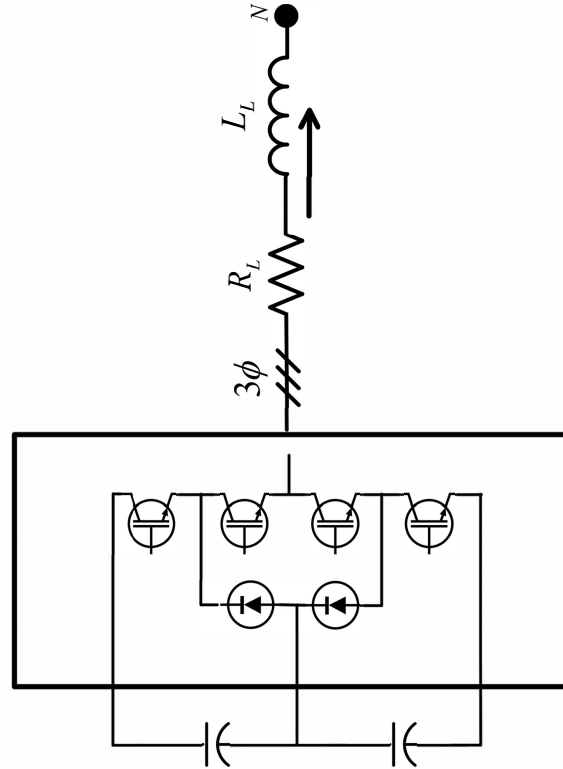
Figure 1. Three phase three-level NPC inverter.

To predict all possible currents $(\vec{i}_{k+1_n})$ in the conventional version of the FS-MPC, all possible voltage vectors related to the switching states should be investigated as $\vec{v}_{k_n}$ in (1). Note that $n = 1, 2, 3, ..., 19$ for a three-phase inverter. Following that, n cost functions should be compared, and the optimum switching state should be chosen using the minimal [17].

$$G_n = \left| \vec{i}_{k+1_n} - \vec{i}^*_{k+1} \right| \tag{3}$$

where $\vec{i}^*_{k+1}$ is the vector of the reference current.

Since predicting the future current for 19 voltage vectors needs a lot of processing power, the simplified FS-MPC is more prevalent for multi-level applications [17]. In this technique, the voltage vector that will deliver the predicted current to the reference value is predicted by (2) as below:

$$\vec{v}^*_{k+1} = \frac{L_L}{t_s} \left(\vec{i}^*_{k+2} - \vec{i}_{k+1} \right) + R_L \vec{i}_{k+1}. \tag{4}$$

Then, the possible voltage vectors will be checked in the following cost function to select the optimum switching state.

$$G_n = \left| \vec{v}_{k+1_n} - \vec{v}^*_{k+1} \right| \tag{5}$$

2.1. Lookup table based triangle detection technique for solution elimination [17]

The space vector is divided into the triangular areas in this method similar to the all area-based methods. To select possible solutions, the triangle in which the reference voltage vector is located is used. The voltage vectors of the determined triangle's vertices are the voltage vectors that will be investigated in the cost function (5). As long as the process of identifying the proper triangle is not lengthy, the idea of using three vectors in the vertices of the triangle reduces processing. The method that is proposed in [17] is the most successful to date. To accomplish a fast determination, the lookup table method and the shift to the first sector are combined. The following is a basic description of this technique:

- **Step1:** The phase angle of the reference voltage vector is calculated.

- **Step2:** The reference voltage vector is shifted to the first sector based on the calculated phase angle. Note that each sector is a $\pi/3 rad$ area.

- **Step3:** The criteria of the lookup table which are based on the slopes of the vectors should be checked, and the related triangle will be determined.

- **Step4:** Based on the found triangle in the first sector, the three possible voltage vectors are found by means of another lookup table via the sector in which the voltage reference is located.

Algorithm 1 Triangular-based lookup table technique for three candidates selection [17].

calculate $\alpha_1 = \frac{1}{\sqrt{3}} v^*_{\beta_{k+1_r}}$

calculate $\alpha_2 = -\frac{1}{\sqrt{3}} \left(v^*_{\beta_{k+1_r}} - \frac{2\sqrt{3}}{3} V_{dc} \right)$

calculate $\alpha_3 = \frac{1}{\sqrt{3}} \left(v^*_{\beta_{k+1_r}} + \frac{2\sqrt{3}}{3} V_{dc} \right)$

calculate $\alpha_4 = -\frac{1}{\sqrt{3}} \left(v^*_{\beta_{k+1_r}} - \frac{4\sqrt{3}}{3} V_{dc} \right)$

if $0 < v^*_{\beta_{k+1_r}} < \frac{\sqrt{3}}{3} V_{dc}$ **then**

  if $\alpha_1 < v^*_{\alpha_{k+1_r}} < \alpha_2$ **then**

    Triangle $\leftarrow T_1$

  else if $\alpha_2 < v^*_{\alpha_{k+1_r}} < \alpha_3$ **then**

    Triangle $\leftarrow T_2$

  else if $\alpha_3 < v^*_{\alpha_{k+1_r}} < \alpha_4$ **then**

    Triangle $\leftarrow T_3$

  end if

else

  Triangle $\leftarrow T_4$

end if

find the related triangle in the correct sector (n_{sec})

use three vertices of the correct triangle

The reference shifting should be performed by the following equation:

$$\vec{v}^*_{k+1_r} = \vec{v}^*_{k+1} e^{-j(n_{sec}-1)\pi/3} \tag{6}$$

The sector in which the reference voltage vector is placed is n_{sec}.

The determination of the related triangle is the main contribution of the method in [17]. Figure. 2 depicts the voltage reference shifting and triangular sections. Algorithm 1 summarizes the method of locating

the corresponding triangle. In this algorithm, four variables α_1 to α_4 should be calculated in every control interval. Calculating these variables increases the computation of the control algorithm. Furthermore, each sector has three triangles, i.e. T_1, T_3, and T_4, each of which is next to a triangle in the other sectors. Therefore, the three selected vectors on the boundary voltages may differ by a small change in the phase angle. This is the common problem in all the triangular-based zoning. In this paper, an alternative zoning technique which is based on vertical areas is proposed.
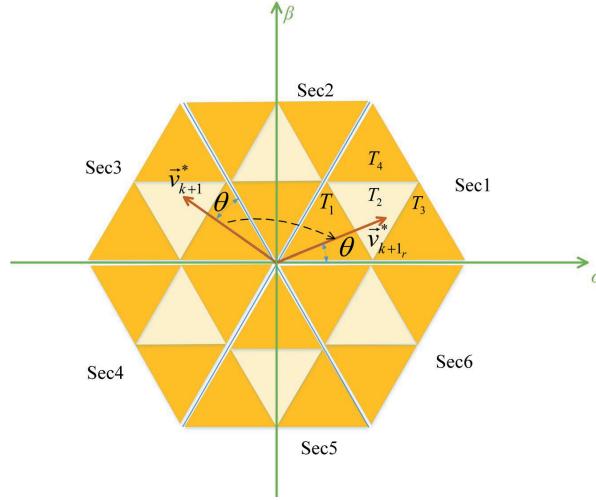

Figure 2. Triangle based voltage vector selection

3. Proposed vertical zoning technique for solution elimination

The triangular technique is based on selecting three adjacent voltage vectors to be examined by the cost function. Each triangle is divided into two areas in this research. The boundary between these two areas will be the height of the triangle. By this method, each right triangle contains two possible voltage vectors. Furthermore, the voltage vectors of the right triangles, which can form a rectangle, are identical. So, they can be merged to a rectangle. Figure 3-a shows the new defined areas in the first sector. It is seen that there are six areas for each sector, i.e. R_1 to R_6. Each zone presents two voltage vector candidates for consideration in the cost function. As a result, the number of possible solutions is decreased from three to two. Since the boundaries of areas are vertical lines, distinguishing the related area needs much less processing power. In other words, α_1 to α_4 do not need to be calculated.

Instead of them, fixed values would be used in the criteria related to the area detection. For this purpose, the direct component of the shifted reference voltage, $v^*_{\alpha,k+1_r}$, should be placed between the ranges of this axis, i.e. 0, $\frac{1}{3}V_{dc}$, $\frac{2}{3}V_{dc}$, V_{dc}, and $\frac{4}{3}V_{dc}$. Also, the quadratic component, $v^*_{\beta,k+1_r}$, should be placed between the related ranges, i.e. 0, $\frac{\sqrt{3}}{3}V_{dc}$ and $\frac{2\sqrt{3}}{3}V_{dc}$. The procedure of finding the correct zone is summarized in Algorithm 2.

When the related zone is determined for the shifted reference voltage vector, the two voltage vectors could be found due to the original sector of the reference voltage, i.e. n_{sec}. The candidate vectors due to the sector and zone are shown in Table 1.

The proposed method outperforms the triangle technique when the voltage reference fluctuations between
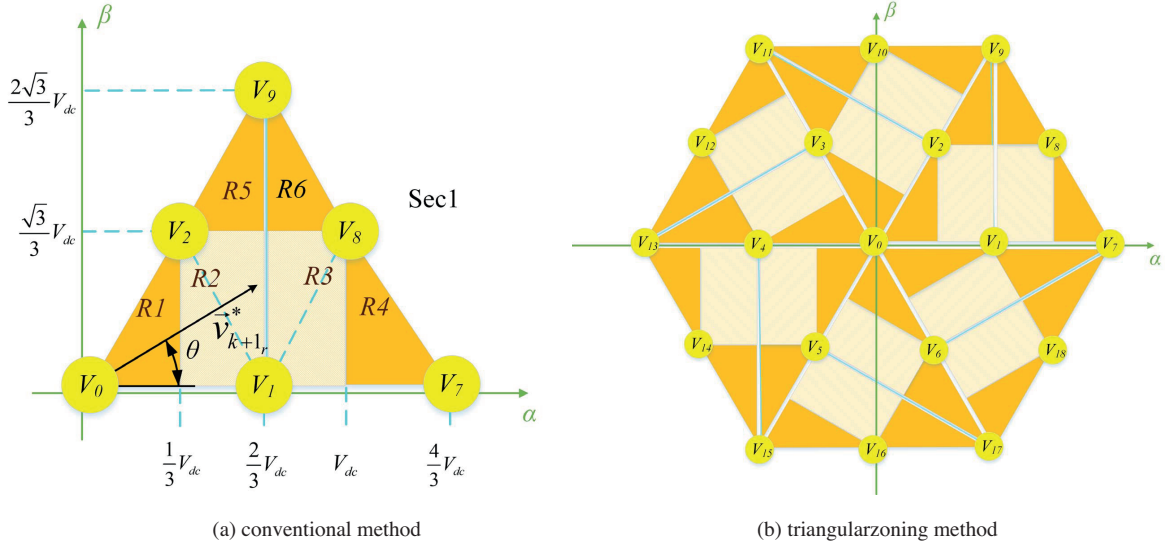
(a) conventional method

(b) triangularzoning method

Figure 3. Proposed vertical positioning technique (a) sector one (b) complete space vector zoning.

Algorithm 2 Proposed vertical zoning technique for two candidates selection

---

if $0 < v^*_{\beta_{k+1_r}} < \frac{\sqrt{3}}{3} V_{dc}$ **then**

  if $0 < v^*_{\alpha_{k+1_r}} < \frac{1}{3} V_{dc}$ **then**

    Zone $\leftarrow R_1$

  else if $\frac{1}{3} V_{dc} < v^*_{\alpha_{k+1_r}} < \frac{2}{3} V_{dc}$ **then**

    Zone $\leftarrow R_2$

  else if $\frac{2}{3} V_{dc} < v^*_{\alpha_{k+1_r}} < V_{dc}$ **then**

    Zone $\leftarrow R_3$

  else if $V_{dc} < v^*_{\alpha_{k+1_r}} < \frac{4}{3} V_{dc}$ **then**

    Zone $\leftarrow R_4$

  end if

else if $\frac{\sqrt{3}}{3} V_{dc} < v^*_{\beta_{k+1_r}} < \frac{2\sqrt{3}}{3} V_{dc}$ **then**

  if $\frac{1}{3} V_{dc} < v^*_{\alpha_{k+1_r}} < \frac{2}{3} V_{dc}$ **then**

    Zone $\leftarrow R_5$

  else

    Zone $\leftarrow R_6$

  end if

end if

find the related zone in the correct sector (n_{sec})

use two vertices of the correct zone

---

two sectors, in addition to requiring less processing power. This case is dominant if the vector fluctuates between the triangles T_2 of two adjacent sectors in the triangular technique. An example could be used to demonstrate this situation. If the reference vector is located in the triangle T_2 of the first sector, the candidates are V_1, V_2, and V_8. The fluctuation of the vector to the same triangle in the second sector changes the candidates to V_2, V_3, and V_{10}, which includes two different vectors from the previous sector. However, if the same scenario happens for the proposed method, i.e. the reference voltage is located in zone R_2 of the first sector, and it fluctuates to the same zone in the second sector, the voltages of the first sector are V_1, and V_2, and they are

V_2, and V_3 for the second sector. It is seen that only one different vector is put to the candidates set. Figure 4 illustrates block diagram of the proposed method.

Table 1. Vectors of the vertical zoning technique.

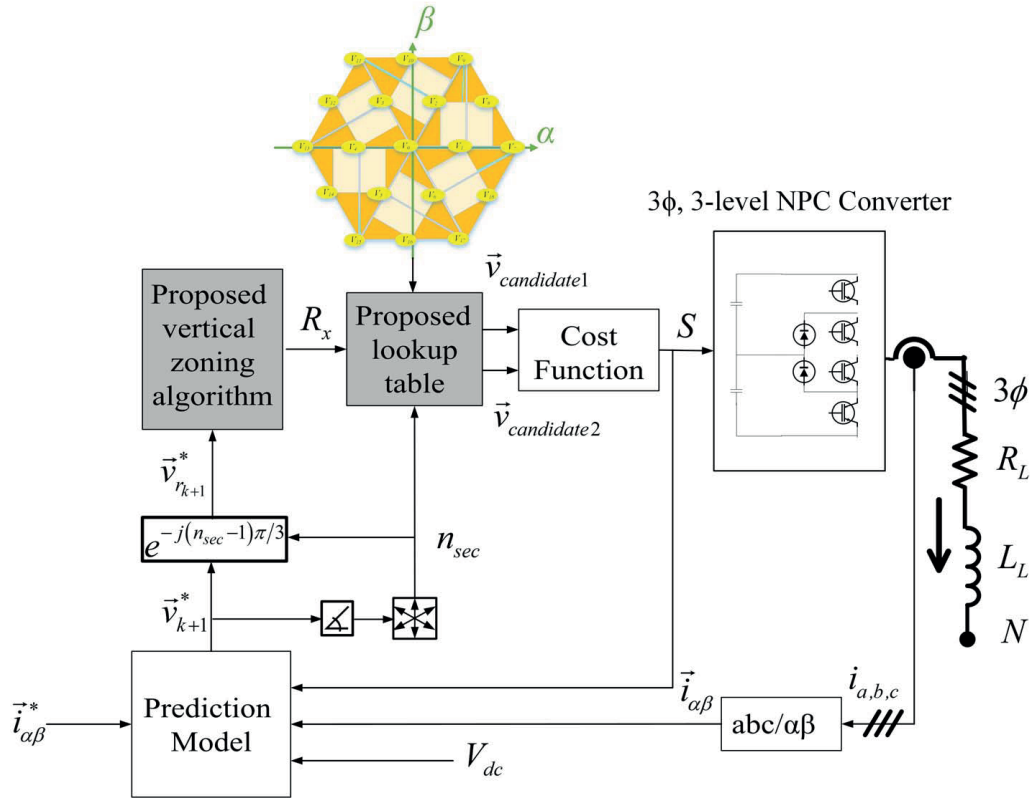| Zone	Sec 1	Sec 2	Sec 3	Sec 4	Sec 5	Sec 6
R_1	V_0,V_2	V_0,V_3	V_0,V_4	V_0,V_5	V_0,V_6	V_0,V_1
R_2	V_1,V_2	V_2,V_3	V_3,V_4	V_4,V_5	V_5,V_6	V_6,V_1
R_3	V_1,V_8	V_2,V_{10}	V_3,V_{12}	V_4,V_{14}	V_5,V_{16}	V_6,V_{18}
R_4	V_7,V_8	V_9,V_{10}	V_{11},V_{12}	V_{13},V_{14}	V_{15},V_{16}	V_{17},V_{18}
R_5	V_2,V_9	V_3,V_{11}	V_4,V_{13}	V_5,V_{15}	V_6,V_{17}	V_1,V_7
R_6	V_8,V_9	V_{10},V_{11}	V_{12},V_{13}	V_{14},V_{15}	V_{16},V_{17}	V_7,V_{18}

Figure 4. Complete block diagram of the proposed FS-MPC.

In the block diagram in Figure 4, the current is measured by current sensors. Then, it is converted to stationary frame and after that, by using (4), $i^*_{\alpha\beta}$, $i_{\alpha\beta}$ and measured voltage of dc link V_{dc}, the reference voltage vector is obtained. The reference voltage of the sector in which it is placed is determined using the angle vector. Then, from the angle, the reference voltage vector has been shifted to the first sector. Algorithm 2 determines the area in which the shifted reference voltage vector is located. From proposed lookup table 1, two candidates are selected based on the reference voltage vector sector number and the shifted reference voltage

vector area number. The selected candidates are placed in the cost function (5), and the selected candidate (S) is selected. For example $v^*_{k+1_r}$ is located in the joined point of R_2, R_3, R_5 and R_6. If the v_α value is greater than $\frac{2}{3}V_{dc}$, the reference voltage vector is in the R_3 or R_6 region, then the V_8 voltage vector is selected. If the v_α value is less than $\frac{2}{3}V_{dc}$, the reference voltage vector is in the R_2 or R_5 region, and the V_2 voltage vector is selected. The flowchart of the proposed method is illustrated in Figure 5.
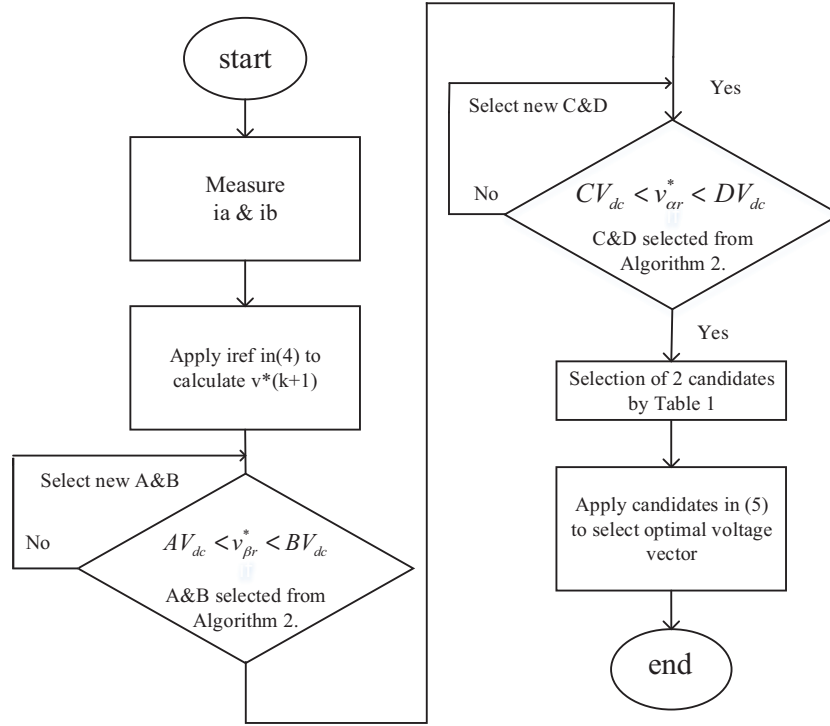

**Figure 5**. Flowchart of the proposed FS-MPC.

4. Simulation results

Simulations by MATLAB are used to assess the suggested predictive current control. The specification of the simulated system, which is used in simulations, is as follows: 1) three-phase three-level NPC inverter with $V_{dc} = 200V$, $I_n = 10A$, $T_s = 100\mu sec$, 2) resistive inductive load with $R_L = 10\Omega$, and $L_L = 10mH$. Simulations are presented for conventional, triangular zoning, and proposed zoning. In the conventional zoning method, all voltage vectors are included in the cost function.

The dynamic responses of three methods are compared in Figure 6. The reference current is changed from $3A$ to $10A$. It's important to note that the nominal current of the simulated structure is $10A$. A new method based on triangular zoning [19] is added to make an accurate comparison between different methods.

Figure 7 shows the two new triangular zoning methods and the proposed method in less time and with more zoom, so that the dynamic characteristics of both methods are comparable.
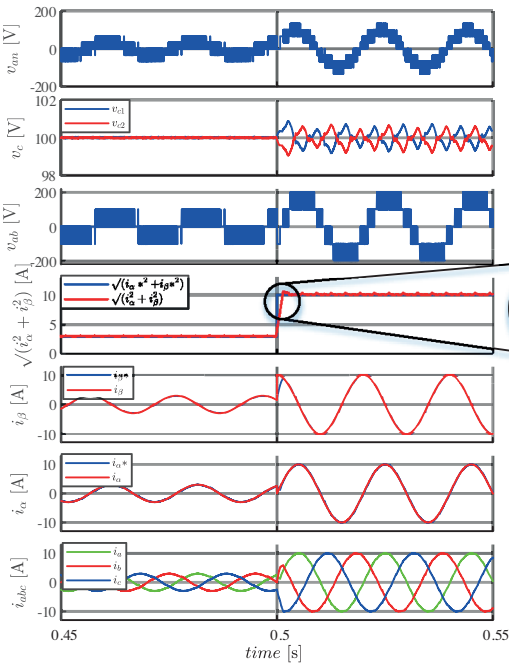
The proposed method, as shown in Table 2, had the same THD as the triangular zoning technique, despite the fact that the number of possible candidates in the proposed technique was reduced from three to two. The conventional method has a better THD due to the greater number of candidates that are put into the
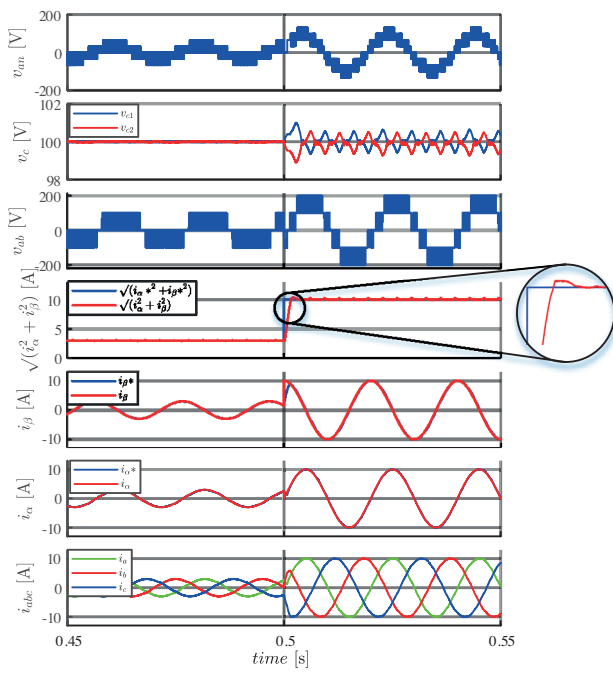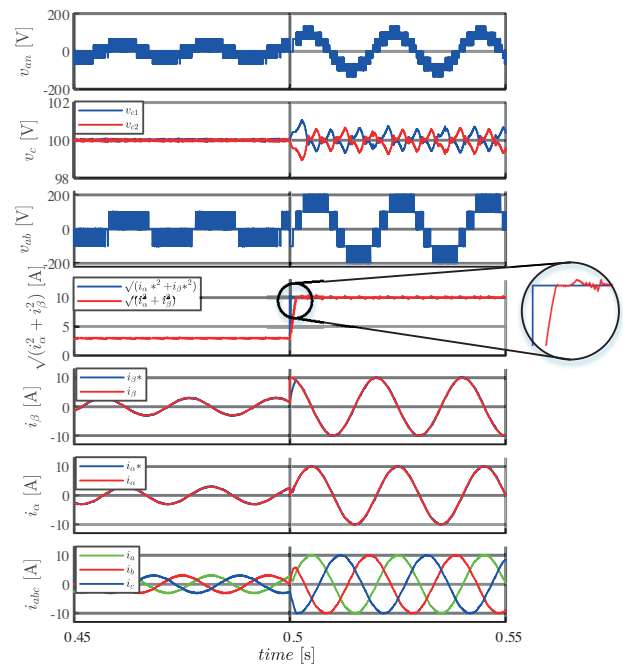
(a) conventional method
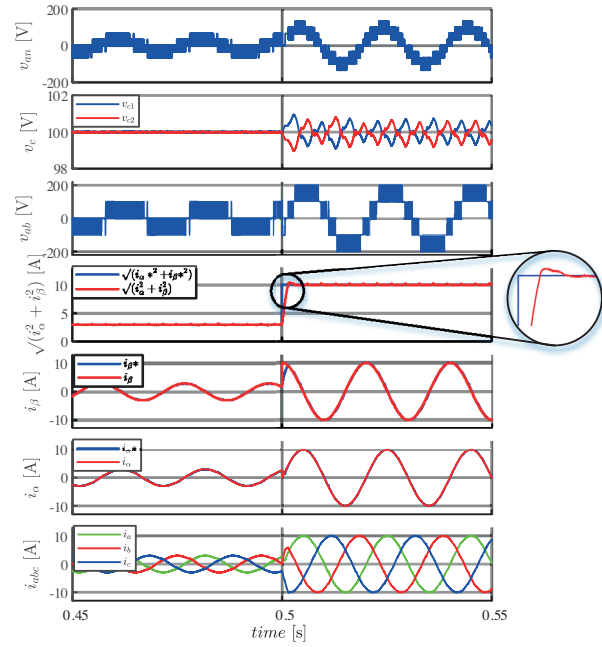
(b) triangular zoning method

(c) new triangular zoning method [19]

(d) proposed vertical zoning method

Figure 6. Dynamic performance comparison during current step response ($I = 3A$ to $I = 10A$).

(a) new triangular zoning method [19]
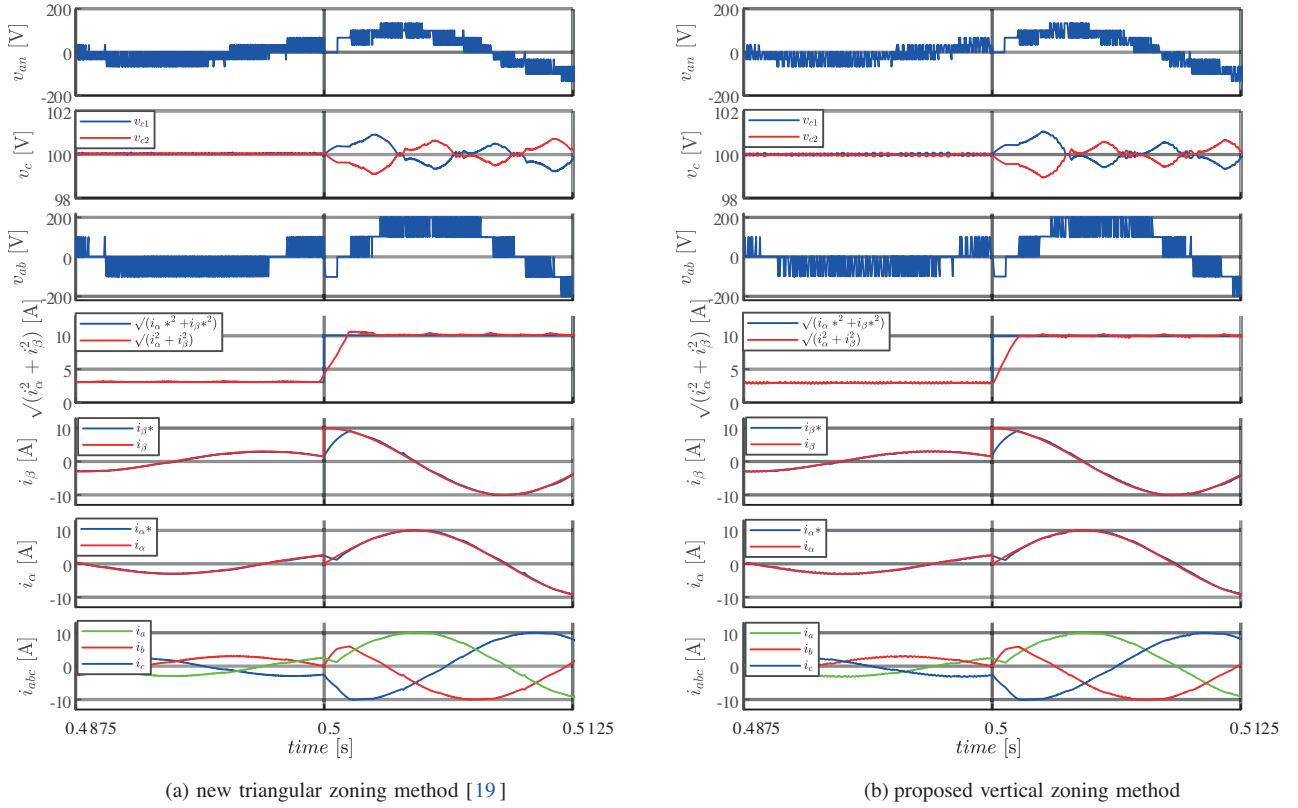
(b) proposed vertical zoning method

Figure 7. Detailed figures of dynamic performance comparison during current step response ($I = 3A$ to $I = 10A$).

cost function. The dynamics of the method is generally due to the precise and rapid selection of areas.

In Figure 8 the selected voltage vector has been shown. The proposed method voltage vectors selecting has been shown in Figure 6. As shown in Table 3, the suggested method's load current tracking error relative to the reference current has improved due to better area selection accuracy. Regarding Figure 6, the dynamic performance of the proposed method has been improved. The rise times of the current vector ($\sqrt{(i_\alpha^2 + i_\beta^2)}$) are shown in Table 4 for all of the methods. Also, there is no overshoot in the step response of the proposed method, while that is shown for that of the triangular and conventional methods.

Table 2. THD of current.

	THD [%]		
Reference current	conventional method	triangular zoning method	proposed vertical zoning method
$I = 10A$	1.25	1.59	1.59
$I = 3A$	3.09	3.57	3.57

The robustness of the proposed method has been studied in Figures 9 and 10. In Figure 9, the load resistance variation is studied. The resistance has increased gradually from $R_L = 10\Omega$, to $R_L = 15\Omega$ during $0.25\ sec$. The resistance is kept at $R_L = 15\Omega$, for $0.1\ sec$ and then decreases gradually to $R_L = 2\Omega$ during
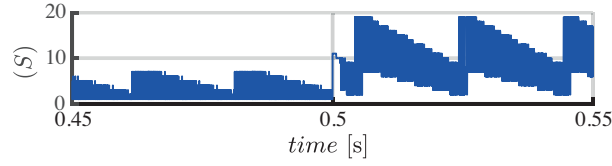
Figure 8. Selected candidates voltage vectors output of cost function (S) ($I = 3A$ to $I = 10A$).

Table 3. Tracking error of the current at $I = 10A$.

Control method	Load current tracking error relative to the reference value [%]
Conventional method	2.1851
Triangular zoning method	2.3098
Proposed vertical zoning method	2.2142

Table 4. quantitative dynamic performance comparison during the step response ($I = 3A$ to $I = 10A$).

Control method	rise time [ms]
Conventional method	1.1
Triangular zoning method	0.8
Proposed vertical zoning method	0.73

0.55 sec. When the resistance changes, the current reference has been kept constant at $I = 8A$. Because of the physical limitation, it is not possible to increase the resistance over 10 Ω and keep the current at nominal current $I = 10A$, and $V_{dc} = 200V$. To provide a variable margin to the load, the current has been set lower than the nominal current at $I = 8A$. Both tables 5 and 6 illustrate the quantized comparisons.

Table 5. Mean value of the current tracking error during load resistance variation at $I = 8A$.

Control method	Reference current and load current tracking error rate [%]
Conventional method	1.0036
Triangular zoning method	0.9575
Proposed vertical zoning method	0.9348

Table 6. Mean value of the THD of current during load resistance variation.

	THD [%]		
Reference current	conventional method	triangular zoning method	proposed vertical zoning method
$I = 8A$	2.85	2.88	2.89

From Table 5, it can be deduced that the current tracking error is smaller for the proposed method during the load resistance variation. Also, in Table 6, it is seen that the proposed method has the better current THD. In Figure 10, in addition to the resistance value, the inductor value has also changed. Both elements are increased from the base value up to 50% and remain constant at this value for 0.1 sec. Then, from the increased value, they are decreased by 110% and reach –60% of the initial value. The reason for this change is
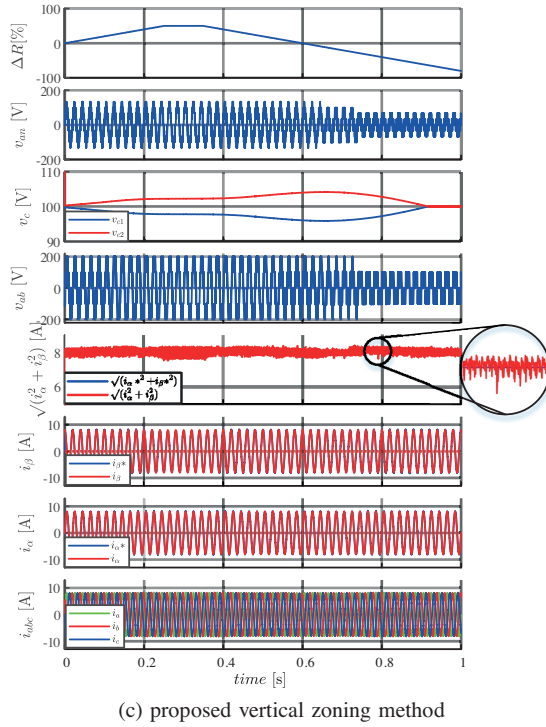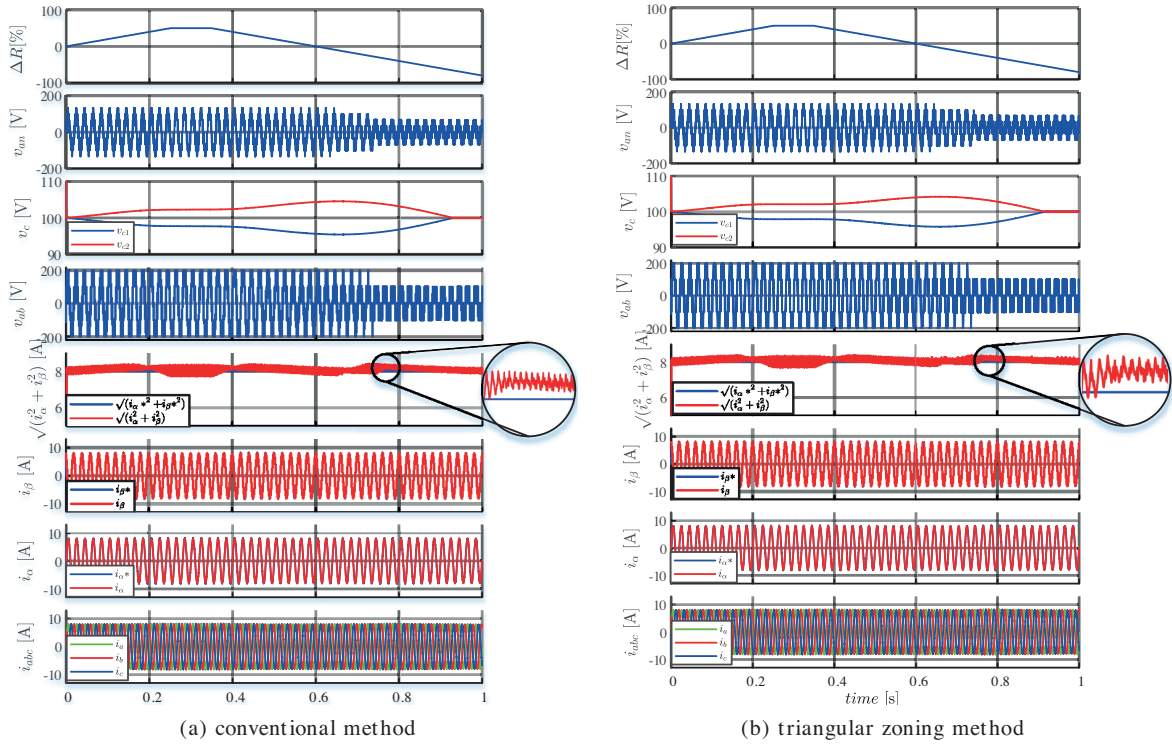
(a) conventional method

(b) triangular zoning method

(c) proposed vertical zoning method

Figure 9. resistance change at $I = 8A$ and $V_{dc} = 200V$.

(a)conventional method

(b) triangular zoing method
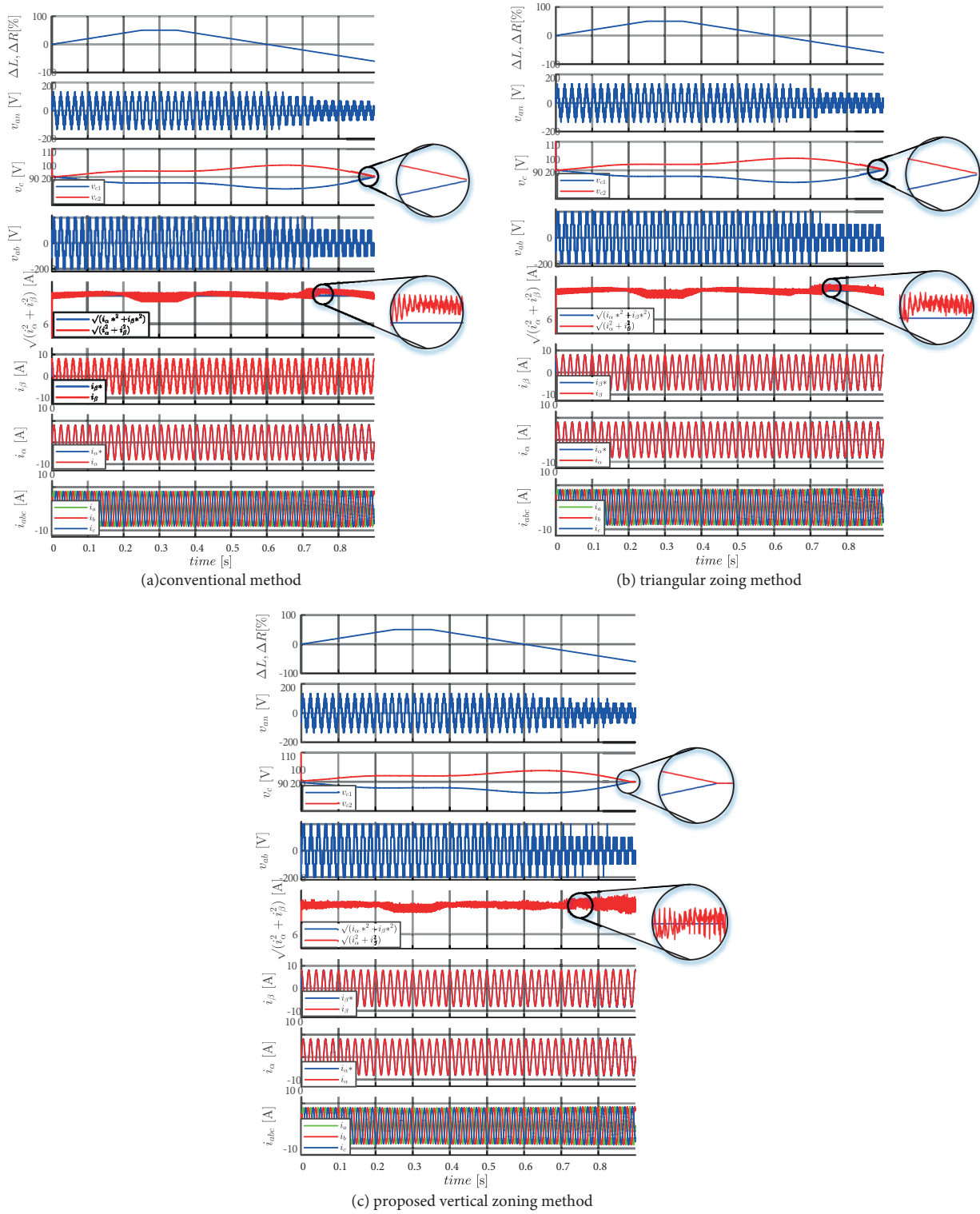

(c) proposed vertical zoning method

Figure 10. Resistance and inductor change at $I = 8A$ and $V_{dc} = 200V$.

the effect of the capacitance-voltage balance by the inductor change. As can be seen from Table 7 and Figure 10, with the simultaneous change of inductor and resistance, the proposed method has a smaller tracking error.

On the other hand, it is clear from Figure 10 that the voltage of the capacitors is balanced in the vertical zoning method 1 *msec* faster than in the triangular zoning method.

In addition to the mentioned comparison between the proposed method, the triangular method and conventional, the execution time is studied as an important advantage of the proposed method. In this paper, by using simulation. First, the total time of the simulation process is calculated using the 'tic toc' code. The number of times that switching is performed during the simulation T_s is specified. The simulation time obtained from the 'tic toc' code time is divided by the number of switching times. The time obtained is the sum of the time of HLT (Hardware Latency Time) and (Task Execution Time) TET. The optimal time is TET, which is obtained by subtracting the HLT time. Table 8 shows the task execution time using simulation. As expected, the computation time in the proposed method has been greatly reduced because of the time associated with one less candidate in addition to the eliminated computational time associated with the slope calculation that was necessary for the triangular method.

Table 7. Current tracking error during resistance and inductance change at $I = 8A$.

Control method	load current tracking error [%]
Conventional method	1.3814
Triangular zoning method	2.0187
Proposed vertical zoning method	1.3795

Table 8. Average computing time using simulation TET

Control method	time [μsec]
Conventional method	33.04
Triangular zoning method	29.25
Proposed vertical zoning method	19.37

A general comparison is shown in Table 9, to make an accurate comparison between all parameters. In this table, a score is given for each of the methods regarding the comparison parameters. The higher score means that the method has a better quality in that parameter. If the parameter in the two methods have the same results, they will have equal scores. As can be seen from Table 9, the proposed method has better results than all other methods.

Table 9. Comparison between all parameters.

Methods	parameters					Final Result
	Voltage balancing of capacitors	Calculation time	Tracking error of current	THD	Dynamic and rise time	
Conventional method	1	1	2	2	1	7
Triangular zoning method	1	2	1	1	2	7
Proposed vertical zoning method	2	3	3	1	3	12

5. Conclusion

The use of the MPC method in multilevel converters increases the number of voltage vectors included in the cost function, and this issue increases the computational burden. A method has been proposed to overcome this shortcoming. In this method, the vertical zoning technique is proposed and applied to a three-level NPC inverter. By this method, in addition to the reduction of the number of candidates, the computation time for recognizing the slope of the boundaries of areas is preserved. By using the proposed method, the voltage balance for the DC link capacitors is achieved. The simulation results showed that the reference current tracking, the load current THD, and the dynamic performance are also improved compared to the prevalent triangular method. The results showed that the computation time has decreased by 33% for the proposed method compared to the triangular method. Note that this method can be applied to the multilevel inverters with higher voltage levels.

References

[1] Marzoughi A, Burgos R, Boroyevich D, Xue Y. Investigation and comparison of cascaded H-bridge and modular multilevel converter topologies for medium-voltage drive application. IECON 2014-40th Annual Conference of the IEEE Industrial Electronics Society 2014, Dallas, TX, USA; 40: 1562-1568. doi: 10.3906/IECON.2014.7048710

[2] Ying J, Gan H. High power conversion technologies & trend. Conference Proceedings 2012 IEEE 7th International Power Electronics and Motion Control Conference - ECCE Asia, Harbin, China, IPEMC 2012; 3: 1766–1770. doi: 10.1109/IPEMC.2012.6259104

[3] Ye Z, Xu Y, Li F, Deng X, Zhang Y. Simplified PWM strategy for neutral-point-clamped (NPC) three-level converter. Journal of Power Electronics 2014; 14 (3): 519–530. doi: 10.6113/JPE.2014.14.3.519

[4] Chokkalingam B, Bhaskar MS, Padmanaban S, Ramachandaramurthy VK, Iqbal A. Investigations of multi-carrier pulse width modulation schemes for diode free neutral point clamped multilevel inverters. Journal of Power Electronics 2019; 19 (3): 702–713. doi: 10.6113/JPE.2019.19.3.702

[5] Taheri A, Zhalebaghi MH. A new model predictive control algorithm by reducing the computing time of cost function minimization for NPC inverter in three-phase power grids. ISA Transactions 2017; 71 : 391–402. doi: 10.1016/j.isatra.2017.07.027

[6] Han J, Li C, Yang T, Han J. Simplified Finite Set Model Predictive Control Strategy of Grid-Connected Cascade H-Bridge Converter. Journal of Control Science and Engineering 2016; 2016 : 1-10. doi: 10.1155/2016/9478387

[7] Vazquez S, Leon JI, Franquelo LG, Rodriguez J, Young HA et al. Model predictive control: A review of its applications in power electronics. IEEE Industrial Electronics Magazine 2013; 8 (1) : 16-31. doi: 10.1109/MIE.2013.2290138

[8] Donoso F, Mora A, Cardenas R, Angulo A, Saez D et al. Finite-Set Model-Predictive Control Strategies for a 3L-NPC Inverter Operating with Fixed Switching Frequency. IEEE Transactions on Industrial Electronics 2018; 65 (5) : 3954–3965. doi: 10.1109/TIE.2017.2760840

[9] Liu X, Wang D, Peng Z. An improved finite control-set model predictive control for nested neutral point-clamped converters under both balanced and unbalanced grid conditions. International Journal of Electrical Power and Energy Systems 2019; 104 (july 2018) : 910–923. doi: 10.1016/j.ijepes.2018.07.046

[10] Li Y, Zhao Y . A Virtual space vector model predictive control for a Seven-Level hybrid multilevel converter. IEEE Transactions on Power Electronics 2020; 36(3) : 3396-3407. doi: 10.1109/TPEL.2020.3015444

[11] Wang Y, Wang X, Xie W, Wang F, Dou M et al. Deadbeat Model-Predictive Torque Control with Discrete Space-Vector Modulation for PMSM Drives. IEEE Transactions on Industrial Electronics 2017; 64 (5) : 3537–3547. doi: 10.1109/TIE.2017.2652338

[12] Norambuena M, Rodriguez J, Zhang Z, Wang F, Garcia C et al. A very simple strategy for high-quality performance of ac machines using model predictive control. IEEE Transactions on Power Electronics 2018; 34 (1) : 794-800. doi: 10.1109/TPEL.2018.2812833

[13] Bahrami A, Norambuena M, Narimani M, Rodriguez J. Model predictive current control of a seven-level inverter with reduced computational burden. IEEE Transactions on Power Electronics 2020; 35 (6) : 5729–5740. doi: 10.1109/TPEL.2019.2952533

[14] Vodola V, Odhano S, Garcia C, Norambuena M, Vaschetto S et al. Modulated model predictive control for induction motor drives with sequential cost function evaluation. IEEE Energy Conversion Congress and Exposition 2019; 2019 : 4911-4917. doi: 10.1109/ECCE.2019.8911870

[15] Siami M, Arab Khaburi D, Rodriguez J. Simplified finite control set-model predictive control for matrix converter-fed pmsm drives. IEEE Transactions on Power Electronics 2018; 33 (3) : 2438–2446. doi: 10.1109/TPEL.2017.2696902

[16] Wang T, Liu C, Lei G, Guo Y, Zhu J. Model predictive direct torque control of permanent magnet synchronous motors with extended set of voltage space vectors. IET Electric Power Applications 2017; 11(8) : 1376-1382. doi: 10.1049/iet-epa.2016.0870

[17] Kim I, Chan R, Kwak S. Model predictive control method for CHB multi-level inverter with reduced calculation complexity and fast dynamics. IET Electric Power Applications 2017; 11 (5) : 784–792. doi: 10.1049/iet-epa.2016.0330

[18] Ja'afari A, Davari SA, Garcia C, Rodriguez J. Computation reduction for balancing the voltages of the DC-link capacitors in 3-level inverter by using redundant switching states. 12th Power Electronics, Drive Systems, and Technologies Conference (PEDSTC) 2021, Tabriz, Iran; 12 : 1–6. doi: 10.1109/PEDSTC52094.2021.9405840

[19] Wang W, Liu Ch, Liu S, Zhao H. Model predictive torque control for dual Three-Phase PMSMs with simplified deadbeat solution and discrete space-vector modulation. IEEE Transactions on Energy Conversion 2021; 36 (2) : 1491–1499. doi: 10.1109/TEC.2021.3052132